EEE6203

Hamish Sams

December 2019

Contents

1 PM machine model in dq reference system (6%)

The electrical response of a SPM machine can be modelled using the equations below (1)-(3).

$$\begin{bmatrix} \mathrm{V}_d \\ \mathrm{V}_q \end{bmatrix} = R \begin{bmatrix} \mathrm{i}_d \\ \mathrm{i}_q \end{bmatrix} + \frac{d}{dt} \begin{bmatrix} \Psi_d \\ \Psi_q \end{bmatrix} + w \begin{bmatrix} \text{-}\Psi_q \\ \Psi_d \end{bmatrix} \tag{1}$$

$$\begin{bmatrix} \Psi_d \\ \Psi_q \end{bmatrix} = \begin{bmatrix} \mathrm{L}_d & 0 \\ 0 & \mathrm{L}_q \end{bmatrix} \begin{bmatrix} \mathrm{i}_d \\ \mathrm{i}_q \end{bmatrix} + \begin{bmatrix} \Psi_m \\ 0 \end{bmatrix} \tag{2}$$

$$T_e = \frac{3p}{2}(\Psi_d i_q - \Psi_q i_d) \tag{3}$$

These equations can be directly translated into simulink as seen in Figure:1.

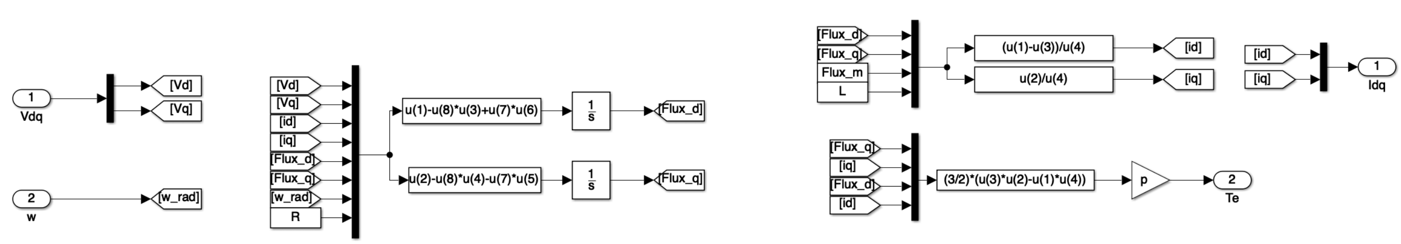

Figure 1: Simulink layout of electrical system design

The mechanical response of an SPM machine can be modeled as below in equation (4).

$$w_m = \int (\frac{T_e - T_m - Bw_m}{J})dt \tag{4}$$

As the rotary speed can be calculated, integrating this gets the rotary displacement $\theta = \int w_{m_{rad}}$ which can also be output. Also converting from radians to rpm can be calculated as $\pi w_{rad} = 30 w_{rpm}$

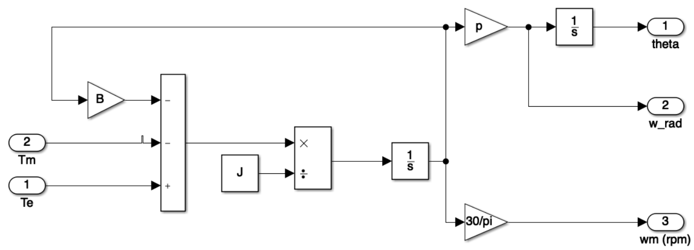

Figure 2: Simulink layout of mechanical system design

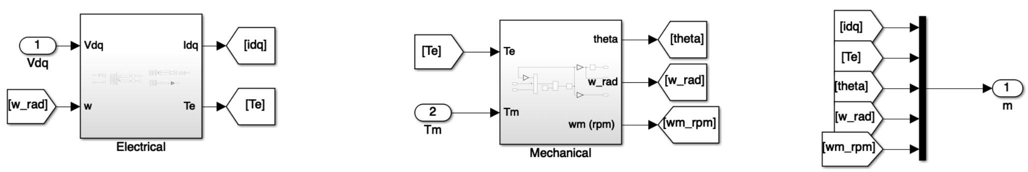

Figure 3: Simulink model of DQ-axis motor using electrical and mechanical blocks

These two systems can be joined together to produce a dq-axis accurate mechanical and electrical motor model as seen in Figure:3.

1.1 PM machine model in ABC reference system (6%)

Using the simplified DQ-ABC and ABC-DQ transforms, know as a Direct-Quadrature-Zero (DQZ) transform (Clarke[1] and Park transform [2]) seen in Equation (5-6) the system can be transformed to and from DQ and ABC frames.

$$K_{CP} = \frac{2}{3} \begin{bmatrix} \cos\theta & \cos\theta - \frac{2\pi}{3} & \cos\theta + \frac{2\pi}{3} \\ \sin\theta & \sin\theta - \frac{2\pi}{3} & \sin\theta + \frac{2\pi}{3} \end{bmatrix} \tag{5}$$

$$K_{CP}^{-1} = \begin{bmatrix} \cos\theta & \sin\theta \\ \cos\theta - \frac{2\pi}{3} & \sin\theta - \frac{2\pi}{3} \\ \cos\theta + \frac{2\pi}{3} & \sin\theta + \frac{2\pi}{3} \end{bmatrix} \tag{6}$$

Using the equations (5-6) can be implemented the simulink shown in Figure:4 and Figure:5 respectively.

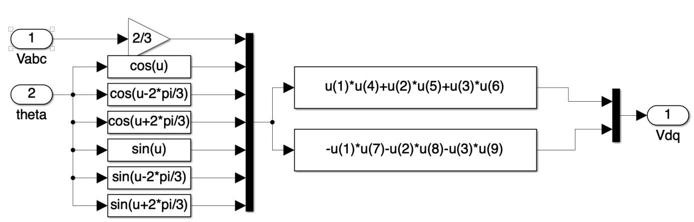

Figure 4: simulink model of ABC-DQ transform

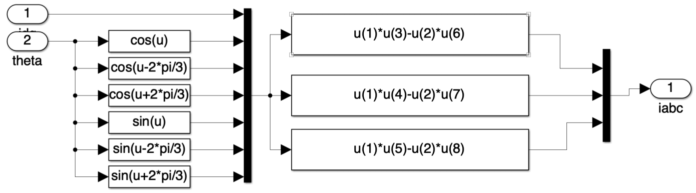

Figure 5: Simulink model of DQ-ABC transform

These DQZ blocks can be implemented on the input and output of the DQ data from the DQ-axis motor model in Figure:3 as shown in Figure:6

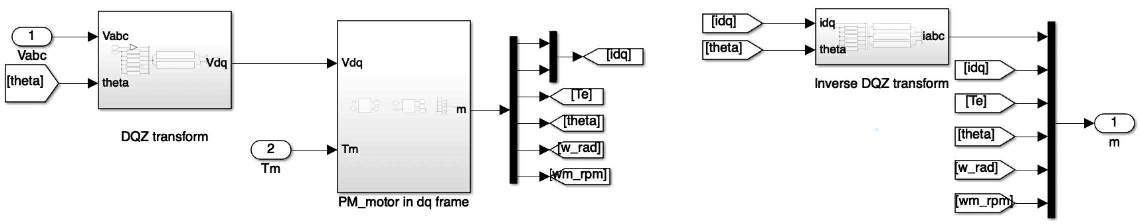

Figure 6: Simulink model of ABC motor model

2 Design dq axis PI current controller with a bandwidth of 800Hz (6%)

For a desired bandwidth β, the corner frequency is given by $\omega_c = 2\pi\beta$, therefore for $\beta = 800$Hz the corner frequency is $\omega_c = 5026.55$rad/s. To define the corner frequency of the PI controller the system must be defined as $\frac{1}{\frac{1}{\omega_c s}+1}$ which may be transformed with the values giving $R\omega_c + \frac{L\omega_c}{s}$ meaning a integral and proportional gain of $L\omega_c$ and $R\omega_c$ respectively.

This PI controller must act on the error in i_{dq} (desired-actual), this is unfortunately coupled due to the Ψ_p and Ψ_d terms present in both PI controllers leading to coupled PI controllers, we therefore must de-couple the PI controllers by removing d and q terms in the q and d PI controllers respectively as seen in equations (7-10).

$$v_d = Ri_d + \frac{d}{dt}(L_d i_d + \Psi_m) - wL_q i_q \tag{7}$$

$$v_q = Ri_q + \frac{d}{dt}L_q i_q - w(L_q di_q d + \Psi_m) \tag{8}$$

$$\frac{d\Psi_d}{dt} = V_d - Ri_d + L_q i_q \tag{9}$$

$$\frac{d\Psi_q}{dt} = V_q - Ri_q - L_d i_d \tag{10}$$

In equation (9-10) the equations add and subtract in the d and q coupling respectively requiring the opposite (subtract and add) these terms as decoupling in the controller. These steps can all be implemented in simulink as seen in Figure: 7.

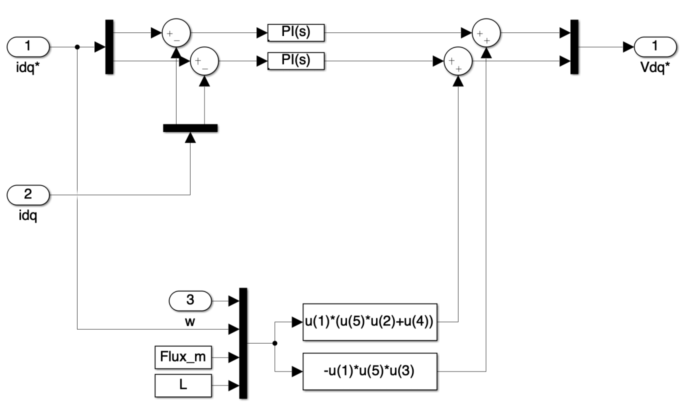

Figure 7: Simulink model of designed PI controller with de-coupling

2.1 Build dq axis current controller with over-modulation protection and anti-winding up (6%)

2.1.1 Over-modulation protection

To protect against over-modulation the PI controller must stop the magnitude of V_{dq} going over V_{max} and below $-V_{max}$ and instead cap at the max value, when not saturating the controller V_{dq} should act linearly. This can be implemented into simulink directly as logic as seen in Figure: 8.

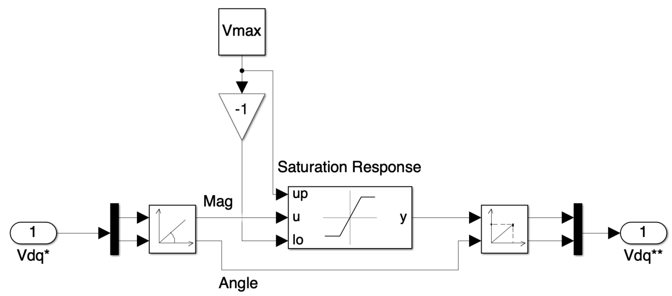

Figure 8: Simulink model of over-modulation protection

2.1.2 Anti-Windup

As the over-modulation block acts non-linearly in the saturation region, if the PI controller integrates within the over-saturation region the integrator will wind-up leading to a large PI integral value to decay once the motor is out of saturation. This is a big problem and as such the PI block must be able to detect if the control system is saturating and if so, stop integrating the error. This can be done by measuring the pre and post control signals, if the pre control voltage is larger than the post overmodulation control signal (aka the overmodulation block is dropping voltage) then oversaturation must be active. This leads to the PI controller seen in Figure: 9.

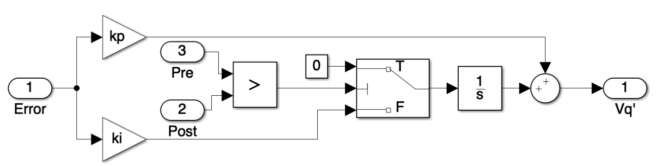

Figure 9: Simulink model of anti-windup PI controller

This PI block is then implemented with pre and post values as seen in Figure:10

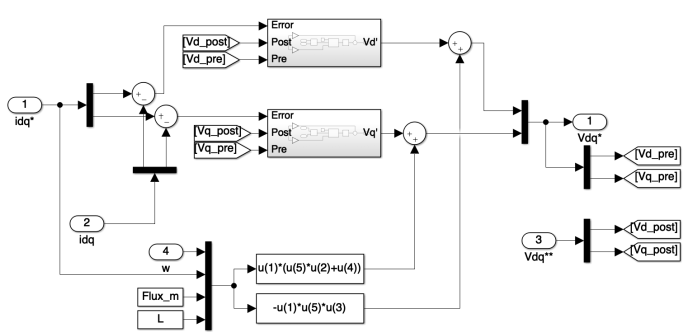

Figure 10: Simulink model of anti-windup PI controller implementation

3 Integrate current controller into the machine model in ABC reference system (6%)

Each component created in the above sections can be added together as seen in Figure: 11. The added system named coordinate transform is an inverse DQZ transform identical to that seen in Figure: 5 instead targeted at converting from dq to abc reference ready to be processed by the abc motor design.

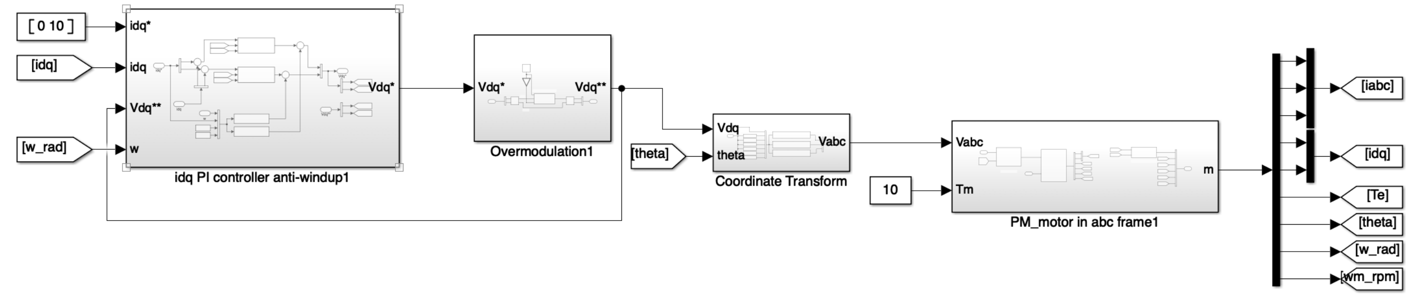

Figure 11: Simulink model of entire motor and controller

4 Perform simulation study of the drive system under torque control mode (10%)

To drive the system under torque control mode the system is initiated with a viscus friction co-efficient of zero and an inertia of infinity (intmax) to drive the motor without controling the speed to reduce any change/decay. Driving an electrical torque of $T_e = 10$ with a step at $t = 5$ to $T_e = 20$ on a load of $T_m = 10$ as seen in Figure: 12. The desired i_{dq} is calculated by converting from torque to current using the relationship $i_{dq} = \frac{T_e}{K_t}$. The i_d value is constantly at 0 as this allows the motor to work with the highest efficiency by having all torque at 90°C to the rotor motion.

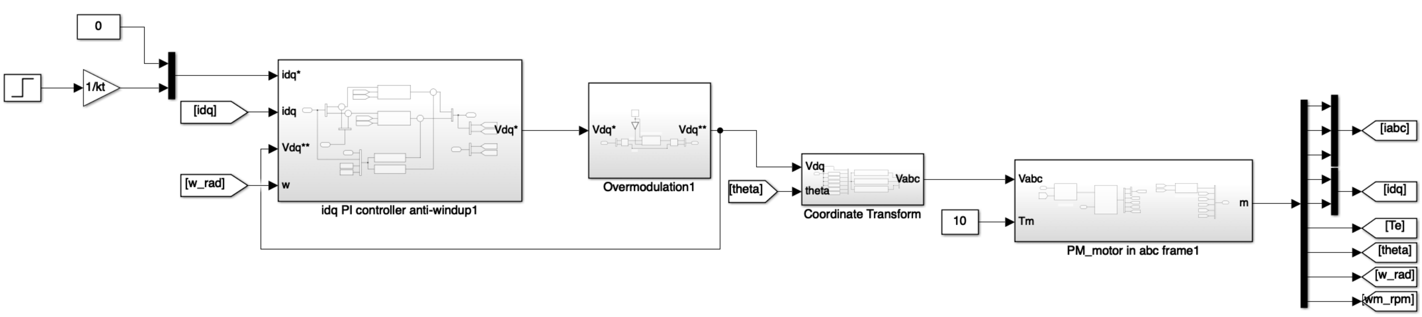

Figure 12: Simulink model of entire motor and controller with a step from $T_e = 10$ to $T_e = 20$ at $t = 5$

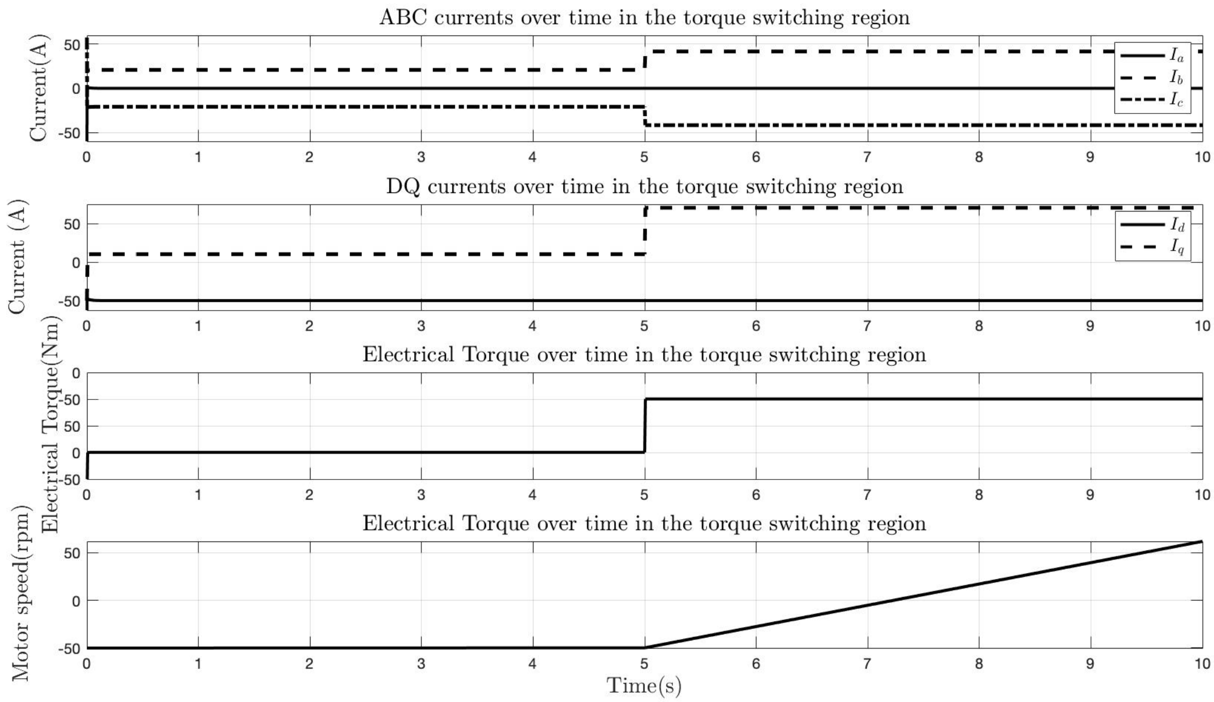

Figure 13: Simulink results of motor design in Figure: 12 with values in Table: 1

Symbol	Value
T_s	$10\mu s$
p	7
L	$344\mu H$
R	$22.2\mu\Omega$
J	realmax('double')
Vdc	$270V$
K_t	0.415
Ψ_m	$39.6mWb$
w_{start}	0
V_{max}	$\frac{V_{dc}}{\sqrt{3}}$
ω_c	$800 \cdot 2\pi$
K_p	$L\omega_c$
K_i	$R\omega_c$
ω_{init}	$\frac{\pi\omega_{start}}{30}$

Table 1: Table of data used in Figure: 13 simulation

In the results seen in Figure: 13 it can be seen that the torque step causes the driving currents i_{abc} to saturate due to the near infinite moment of inertia of the rotor leading to a near DC signal being output on the b and c phases pulling and pushing the rotor as much as possible. Even though the rotor is near infinitely heavy, the motor still rotates, despite being impossibly small due to no static friction.

5 Design speed control loop and establish speed control system model (10%)

To create a pre current controller speed controller PI, the system must first calculate the error requiring a desired and actual speed, this speed will be fed into the 50Hz tuned PI block. This PI will then directly drive the current controller previously discussed and used. Following similar derivation to that in section 2 the P and I gains are calculated below in Figure: 14 and equations (11-15) giving $K_p = \frac{2 \cdot 2\pi f_c J}{K_t}$ and $K_i = \frac{2 \cdot (2\pi f_c)^2 J}{K_t}$. The K_p is multiplied by 2 compared to $\sqrt{2}$ as a critically damped system is used to reduce overshoot of the device, for a faster response time $\sqrt{2}$ could be used. Represented as an

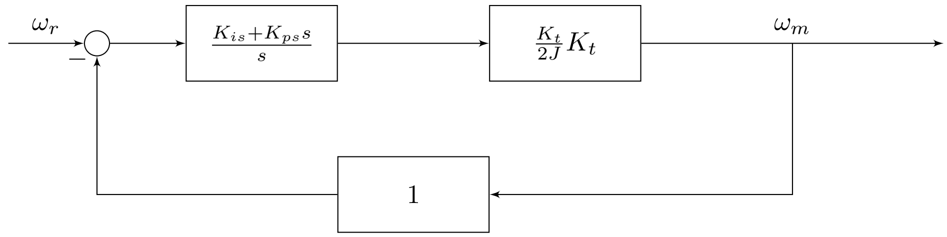

Figure 14: Speed controller feedback loop

equation:

$$\frac{\omega_m}{\omega_r} = \frac{\frac{(K_i+K_pS)K_t}{S^2J}}{1+\frac{(K_i+K_pS)K_t}{S^2J}} \tag{11}$$

In second order standard form, assuming the numerator zero is negligible given $K_p << K_i$:

$$\frac{\omega_m}{\omega_r} = \cdot \frac{\frac{K_iK_t}{J}}{S^2+\frac{K_pK_t}{J}S+\frac{K_iK_t}{J}} \tag{12}$$

Compare to standard second order:

$$\frac{\omega_m}{\omega_r} = \frac{\omega_n^2}{S^2+2\zeta\omega_nS+\omega_n^2} \tag{13}$$

Giving:

$$\omega_n^2 = \frac{K_iK_t}{J} \qquad 2\zeta\omega_n = \frac{K_pK_t}{J} \tag{14}$$

Finally:

$$K_p = \frac{2\cdot 2\pi f_cJ}{K_t} \qquad K_i = \frac{2\cdot(2\pi f_c)^2J}{K_t}. \tag{15}$$

This is then implemented as seen in Figure: 15 as a speed controller block being driven as seen in Figure: 16. In this PI an output saturation current is applied with the output saturation section of upper and lower limit as specified in Table: 2.

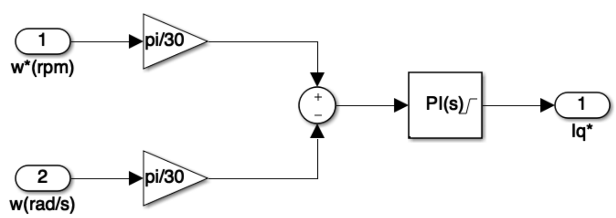

Figure 15: Simulink speed controller PI block

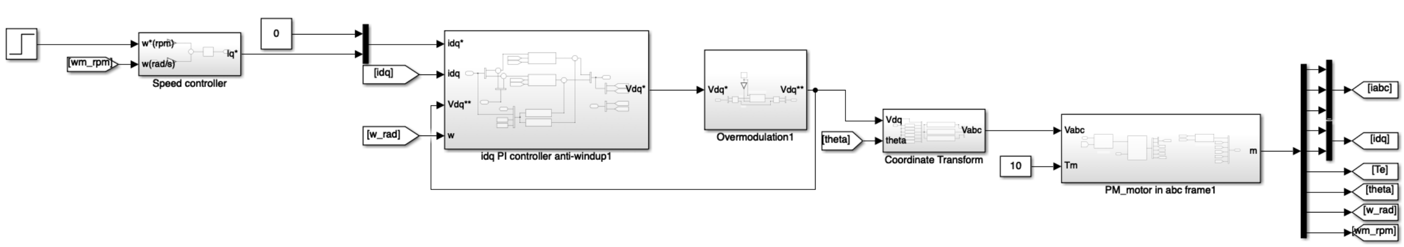

Figure 16: Simulink implementation of speed controller PI block

6 Perform simulation study of close loop speed control of the drive system (10%)

The following results are given by the simulation in the speed controlled motor model seen above in Figure: 16.

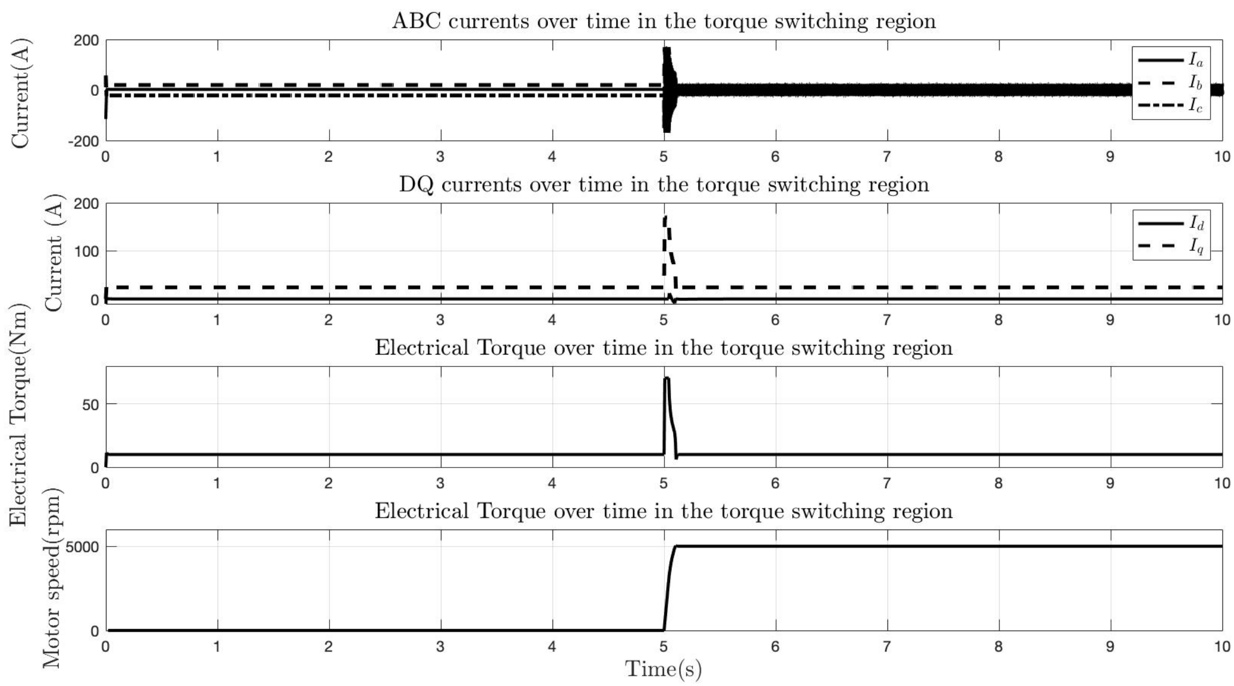

Figure 17: Simulink implementation of speed controller PI block results

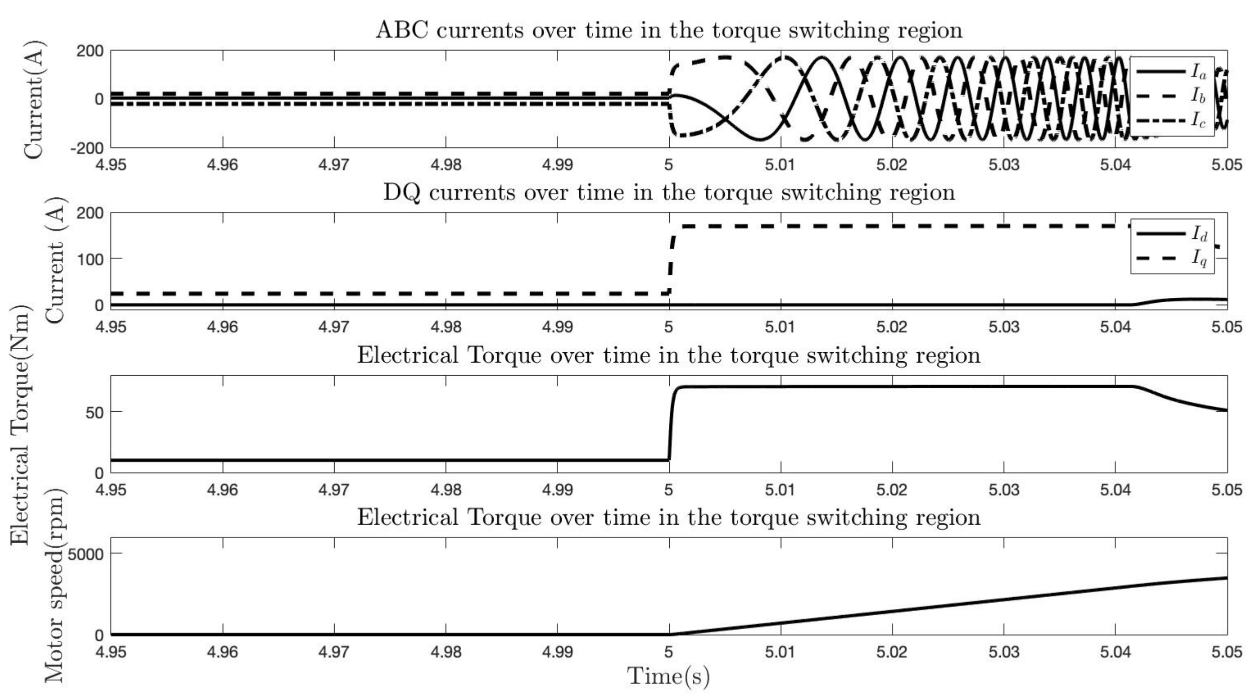

Figure 18: Simulink implementation of speed controller PI block results in speed switching region

The results seen in Figure: 17 show the results at the switching instant from zero to 5000 rpm, as critical damping was used for the speed controller the system shows nearly no signs of overshoot above the 5000 rpm target, the system in this instant controls the i_{abc} currents increasing the speed, a closer view showing the sine waves speeding up as the rotor accelerates can be seen at the top of Figure 18. After the motor has reached the target velocity the motor can be seen to match the magnitude before the switching, this is the voltage required to counteract the constant reverse torque keeping the machine at 5000 rpm. These i_{abc} currents can be seen in the DQ-frame in the second graph, in DQ it is desired for i_d to be zero with the i_q current driving the rotational force, this is almost exactly what is seen in Figure: 17 and 18 with a slight change in i_d due to the voltage error being required to drive the PI correction. The dipping seen in the torque and current graphs is due to the PI controller driving the system for low overshoot.

7 An inverter model with space vector modulation is integrated into the drive system model and operation demonstrated (10%)

8 Appendices

Specification	Value
Machine Topology	Surface Mount Permanent Magnet
Number of pole-pairs(p)	7
Connection	Star
Continuous power	$5kW$
Peak Power	$10kW$
Phase resistance at 120°C (R)	$22.2m\Omega$
Synchronous inductance (L)	$0.344mH$
Flux linkage per phase (mWb) (Ψ_m)	$39.6mWb$
Torque constant(K_t)	$0.415\frac{Nm}{A_p}$
Back-emf constant	$0.277\frac{V_ps}{rad}$
Base speed	$1350rpm$
Maximum speed	$5500rpm$
Continuous current	$\frac{85}{60.5}\frac{A_p}{rms}$
Maximum current	$\frac{170}{121}\frac{A_p}{rms} >$ 2minutes
Moment of inertia (J)	$0.008kgm^2$
DC link voltage (V_{dc})	$270V$

Table 2: Table of motor specification

Symbol	Description
i_{dq}	Rotor frame currents
V_{dq}	Rotor frame voltages
Ψ_{dq}	Rotor frame flux linkages
Ψ_m	Magnet flux linkage
p	Pole pairs
R	Armatur resistance
w	Electrical angular speed
T_e	Electromagnetic torque
L_{dq}	dq-axis inductances
w_m	Mechanical speed
T_m	Mechanical load torque
B	Viscous friction coefficient
J	Inertia
K_t	Torque constant

Table 3: Table of symbols

9 References

[1] WC Duesterhoeft, Max W Schulz, and Edith Clarke. Determination of instantaneous currents and voltages by means of alpha, beta, and zero components. *Transactions of the American Institute of Electrical Engineers*, 70(2):1248–1255, 1951.

[2] Robert H Park. Two-reaction theory of synchronous machines generalized method of analysis-part i. *Transactions of the American Institute of Electrical Engineers*, 48(3):716–727, 1929.